Journal of Power Sources 180 (2008) 484–490

Contents lists available at ScienceDirect

Journal of Power Sources

journal homepage: www.elsevier.com/locate/jpowsour

Effects of electroless deposition conditions on microstructures of cobalt–phosphorous catalysts and their hydrogen generation properties in alkaline sodium borohydride solution

KwangSup Eom, KeunWoo Cho, HyukSang Kwon*

Department of Materials Science and Engineering, Korea Advanced Institute of Science and Technology, Guseong-dong 373-1, Yuseong-gu, Daejeon 305-701, Republic of Korea

ARTICLE INFO

Article history:
Received 19 October 2007
Received in revised form 31 December 2007
Accepted 29 January 2008
Available online 10 March 2008

Keywords:
Sodium borohydride
Cobalt–phosphorous catalyst
Hydrogen generation rate
Hydrolysis
Electroless deposition
Microstructure

ABSTRACT

Cobalt–phosphorous (Co–P) catalysts with a high hydrogen generation rate in alkaline sodium borohydride ($NaBH_4$) solution are developed by electroless deposition. The microstructures of the Co–P catalysts and their catalytic activities for hydrolysis of $NaBH_4$ are analyzed as a function of the electroless deposition conditions such as the pH and temperature of the Co–P bath. The electroless-deposited Co–P catalysts are composed of nano-crystalline Co and amorphous Co–P. The size of the nano-crystalline Co particles dispersed in amorphous Co–P matrix depends largely on the electroless deposition conditions. Moreover, Co–P catalysts with finer crystalline Co exhibit a higher hydrogen generation rate. In particular, the Co–P catalysts formed in a pH 12.5 bath at 60–70 °C exhibit the best hydrogen generation rate of 3300 ml min^{-1} g^{-1}-catalyst in 1 wt.% NaOH + 10 wt.% $NaBH_4$ solution at 30 °C, which is 60 times faster than that obtained with a Co catalyst.

1. Introduction

Proton exchange membrane fuel cells (PEMFCs) using hydrogen as a fuel are attractive alternative power sources for vehicles and portable electronic devices due to their high efficiency, high power density, and zero emission of environment pollutants. In order to utilize PEMFCs successfully, it is essential to develop a safe and convenient hydrogen storage and production system.

During the past few decades, many efforts have been made to develop hydrogen storage systems with high capacity using high pressure vessels [1], metal hydrides [2,3] and carbon nanotubes [4]. Despite this work, the hydrogen storage density in terms of specific energy density is still not sufficient for commercial applications. Recently, chemical hydrides such as $NaBH_4$, $LiBH_4$, NaH and $NaAlH_4$ have received considerable attention as more promising hydrogen storage materials. Among them, sodium borohydride ($NaBH_4$) provides safe and practical means of hydrogen storage and production at an economical cost compared with other chemical hydrides [5–15].

$NaBH_4$ offers a high hydrogen storage density up to 10.8 wt.%, and is able to produce hydrogen by a hydrolysis reaction:

$$NaBH_4 + 2H_2O = NaBO_2 + 4H_2, \quad \Delta H = 217\ \text{kJ} \tag{1}$$

The hydrolysis rate of $NaBH_4$ is very sensitive to pH, and decreases with increase in pH [5]. This means that the hydrolysis of $NaBH_4$ is significantly restrained in an alkaline solution. Therefore, an alkaline $NaBH_4$ solution is able to store hydrogen safely and stably at room temperature. For hydrogen generation from the alkaline $NaBH_4$ solution, suitable catalysts are required to promote the hydrolysis of $NaBH_4$. In particular, noble metal catalysts such as Ru and Pt have been reported to exhibit high catalytic activity for the hydrolysis of $NaBH_4$ [6–8]. These noble metal catalysts are very expensive, however, and it is therefore necessary to develop an economical alternative catalyst with high catalytic activity. To solve this problem, various catalysts based on transition metals such as Co, Ni, Co–B and Ni–B have been studied [9–14]. Above all, Co–B catalysts exhibit the highest activity for $NaBH_4$ hydrolysis equivalent to that of noble metal catalysts. Nevertheless, because most of the Co–B catalysts have been prepared using a chemical reduction method without a substrate, their ability to be used repeatedly in alkaline $NaBH_4$ solution has proven to be a challenge. Accordingly, the development of Co-based catalysts with not only high catalytic activity but also strong adhesion between a substrate and the catalyst material is required for more practical use. Cho and Kwon [15]

* Corresponding author. Tel.: +82 42 869 3326; fax: +82 42 869 3310.
E-mail address: hskwon@kaist.ac.kr (H. Kwon).

0378-7753/$ – see front matter © 2008 Elsevier B.V. All rights reserved.
doi:10.1016/j.jpowsour.2008.01.095

reported that Co–P catalysts electrodeposited on a copper substrate gave 18 times higher catalytic activity for $NaBH_4$ hydrolysis than Co catalysts. Moreover, contrary to the powdery catalysts formed by a chemical reduction method, the electrodeposited Co–P catalysts can be used repeatedly due to strong adhesion between the Cu substrate and the Co–P electrodeposits. Unfortunately, it is difficult to electrodeposit uniformly a Co–P layer on a porous substrate such as a foam metal due to a relatively low throwing power. In this regard, electroless deposition may be an alternative for achieving a uniform catalyst layer on a porous substrate with large surface area. Furthermore, electrodeposited Co–P catalysts can be only formed on a conducting substrate such as metal, but electroless-deposited Co–P catalysts have an advantage in that they can be formed uniformly on polymer and ceramic substrates as well as metal. Nevertheless, the effects of electroless-deposited Co–P catalysts on the hydrolysis of $NaBH_4$ have not yet been studied.

In the present work, the influence of electroless deposition conditions such as the pH and the temperature of the Co–P bath on the microstructures of the Co–P catalysts and their hydrogen generation properties in alkaline $NaBH_4$ solution are examined in order to develop Co–P catalysts with excellent efficiency for $NaBH_4$ hydrolysis.

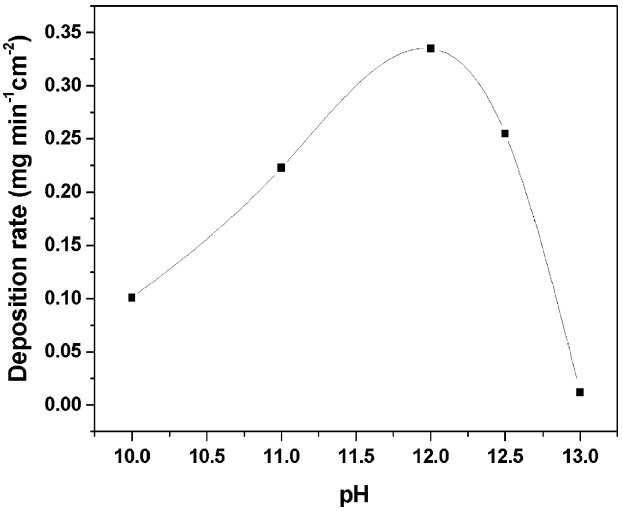

Fig. 1. Effects of pH in electroless Co–P deposition bath on deposition rate.

2. Experimental

2.1. Preparation of catalysts

A Cu sheet with an exposed surface area of 16 cm^2 was used as a substrate for Co–P electroless deposition. The sheet was catalyzed in a $SnCl_2$ (1 g L^{-1}) + HCl (1 ml L^{-1}) solution for 3 min at 25 °C, accelerated in a $PdCl_2$ (0.1 g L^{-1}) + HCl (1 ml L^{-1}) solution for 1 min at 25 °C, and washed with distilled water prior to the electroless deposition.

The electroless deposition of Co–P was conducted in a chloride-based solution that was agitated with a magnetic stirrer at 100 rpm. The bath composition was 0.1 M $CoCl_2{\cdot}6H_2O$, 0.6 M NH_2CH_2COOH and 0.8 M $NaH_2PO_2{\cdot}H_2O$, as employed by Tarozaite et al. [16]. The pH of the Co–P bath was varied from 10 to 13 by the addition of NaOH, and temperature was controlled from 50 to 90 °C by means of a thermostat. The surface morphologies and compositions of the Co–P catalysts were analyzed with scanning electron microscopy (SEM), energy dispersive spectroscopy (EDS), X-ray diffraction (XRD), and transmission electron microscopy (TEM).

2.2. Measurement of hydrogen generation rate

To examine the effects of the electroless deposition conditions on the hydrogen generation properties of the Co–P catalysts, hydrogen generation tests were performed in 50 ml 1 wt.% NaOH + 10 wt.% $NaBH_4$ solution at 30 °C. The volume of generated hydrogen gas was measured by a gas flow meter. The reactor was immersed in a water bath to stabilize the temperature, and no stirring was carried out in the reactor.

3. Results and discussion

3.1. Effects of pH in Co–P bath

In order to control the deposited weight of the Co–P catalysts, the deposition rate from the Co–P bath at 80 °C was examined as a function of pH; the results are presented in Fig. 1. As the bath pH is increased from 10 to 12, the deposition rate of the Co–P catalysts increases from 0.101 to 0.335 mg min^{-1} cm^{-2}. When the pH is further increased to pH 13, however, the deposition rate decreases. Especially, in the case of the pH 13 bath, the Co–P catalysts reduce spontaneously, even without immersion of the Cu substrate, and precipitated in the bath. This resulted in a significant decrease in their deposition rate to 0.012 mg min^{-1} cm^{-2}.

The surface morphologies of the electroless-deposited Co–P catalysts largely depend on the bath pH, as shown in Fig. 2. The weight of the Co–P deposits is 1.25 mg cm^{-2}. In the Co–P bath of pH 10, fine and ridge-shaped Co–P crystals are formed on the Cu substrate and are arranged randomly. Moreover, coarse Co–P crystals with polyhedral shape as well as fine crystals are observed locally. As the bath pH was increased to 12.5, the number of coarse Co–P crystals increases and their shape gradually transforms from a polyhedral to a spherical shape. It is notable that micro-cracks are present on the fine Co–P layer as this indicates that high residual stress exists within the layer [17]. The number of course Co–P crystals decreases drastically and rough surfaces with micro-cracks are formed with further increasing the bath pH to 13. Fig. 2(f) shows the cross-section of the Co–P deposited in the bath of pH 12.5. This clearly shows that the Co–P deposit consists of a duplex layer structure of outer spherical Co–P particles and an inner flat Co–P layer. From EDS analysis, it is found that the Co–P catalysts deposited at pH 10–13 contains 8–11 at.% P, which indicates that the chemical composition of the Co–P catalysts is not dependent on the pH of the Co–P bath.

For all the Co–P catalysts, the (1 0 0) and (1 0 1) planes of the hexagonal close packed (HCP) Co phase are detected, and the sharp peaks demonstrate that the Co deposit is a crystalline structure. The peak related to the Co and P compound phase is not detected, which indicates that the compound has an amorphous structure. A TEM image and an electron diffraction pattern of a Co–P catalyst formed on Cu in the Co–P bath at pH 12.5 are presented in Figs. 3 and 4, respectively. The data show that the Co–P catalyst consists of two different phases: the grey regions are associated with the amorphous phase of the Co and P compound, and the dark spots are nano-crystalline Co particles of less than 10 nm in size. Thus, it is found that the electroless-deposited Co–P catalysts consist of nano-crystalline Co particles precipitated from the amorphous Co–P matrix phase.

In order to investigate further the effects of bath pH on the microstructure of the electroless-deposited Co–P catalysts, the average crystalline size of Co phase in the Co–P catalysts was calculated based on the Scherrer's equation (Eq. (2)) [18] by measuring the breadth at half intensity for the HCP Co(1 0 0) and Co (1 0 1)

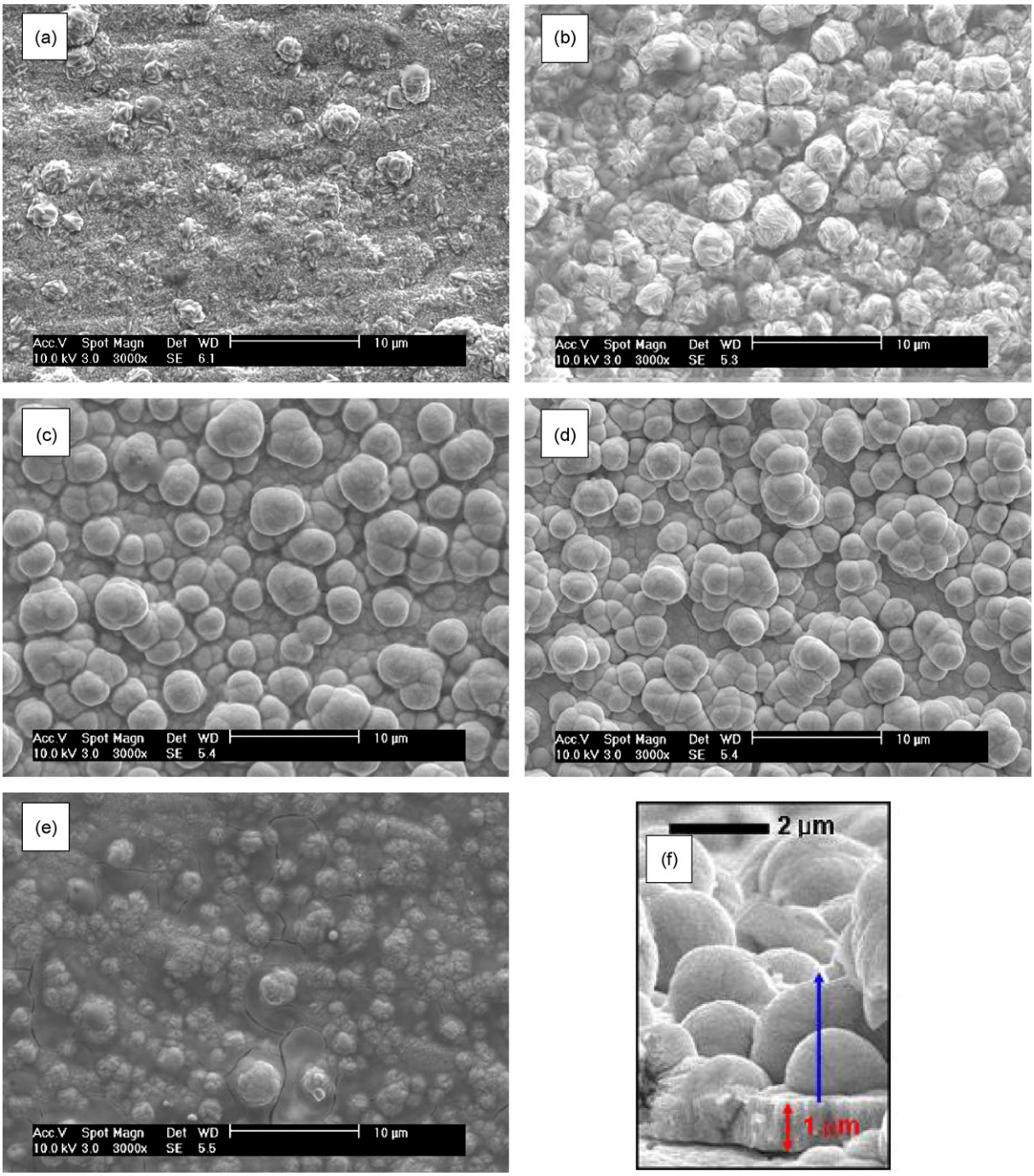

Fig. 2. SEM surface images of Co–P catalysts electroless deposited from Co–P bath of (a) pH 10, (b) pH 11, (c) pH 12, (d) pH 12.5, and (e) pH 13 at 80 °C; (f) a cross-section image of (d).

peaks shown in Fig. 5. The results are presented in Table 1:

$$t = \frac{0.9\lambda}{B\cos\theta} \quad (2)$$

In Eq. (2), t is the particle size (crystal thickness), B is the breadth at half intensity of the peak, θ represents Bragg angle of the peak, and λ denotes the X-ray wavelength. As the bath pH is increased from 10 to 12.5, the nano-crystalline Co size in the Co–P catalysts decreases significantly from 16.9 to 5 nm. When the bath pH is further increased to 13, however, the size abruptly increases to 17.7 nm. Thus, it is concluded that the bath pH may be a critical factor in determining the hydrogen generation properties of the electroless-deposited Co–P catalysts, because the catalytic activity of the amorphous Co–P compound for the hydrolysis of $NaBH_4$ is much higher than that of crystalline Co [15].

Table 1
Size of Co crystals in Co–P catalysts electroless deposited from Co–P bath of pH 10–13 at 80 °C

pH in Co–P bath	Average Co crystal size (nm) measured from HCP Co(1 0 0), (1 0 1) peaks by Scherrer's equation
10	16.9
11	14.5
12	7.9
12.5	5.0
13	17.7

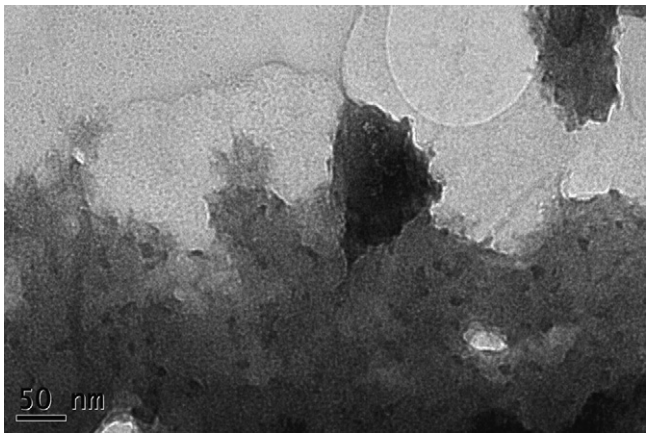

Fig. 3. TEM image of Co–P catalysts electroless deposited from Co–P bath of pH 12.5 at 80 °C (dark spots: Co crystals; grey region: amorphous Co–P).

Fig. 6 shows the effects of the bath pH on the hydrogen generation properties of the electroless-deposited Co–P catalysts in a solution of 1 wt.% NaOH and 10 wt.% $NaBH_4$ at 30 °C. As the pH of the Co–P bath is increased from 10 to 12.5, the hydrogen generation rate of the Co–P catalysts increases from 260 to 3100 ml min^{-1} g^{-1}-catalyst. With a further increase in the pH to 13, however, the hydrogen generation rate decreases dramatically to 170 ml min^{-1} g^{-1}-catalyst. In our previous study [15], it was reported that a Co catalyst in the same solution of 1 wt.% NaOH and 10 wt.% $NaBH_4$ at 30 °C gave a hydrogen generation rate of 52 ml min^{-1} g^{-1}-catalyst. Thus, the Co–P catalyst that is electroless deposited in a pH 12.5 bath yields a hydrogen generation rate that is 60 times higher than with a Co catalyst.

From Table 1 and Fig. 6, it is found that the microstructures and hydrogen generation properties of the electroless-deposited Co–P catalysts depend largely on the pH of the Co–P bath. It is significant that as the size of the nano-crystalline Co in the Co–P catalysts decreases, the catalytic activity increases. In particular, the Co–P catalyst electroless deposited in a bath at pH 12.5 consists of the smallest Co nano-crystals (average 5 nm diameter) precipitated from the amorphous Co–P phase, and shows the best hydrogen generation rate of 3100 ml min^{-1} g^{-1}-catalyst in a solution of 1 wt.% NaOH and 10 wt.% $NaBH_4$ at 30 °C.

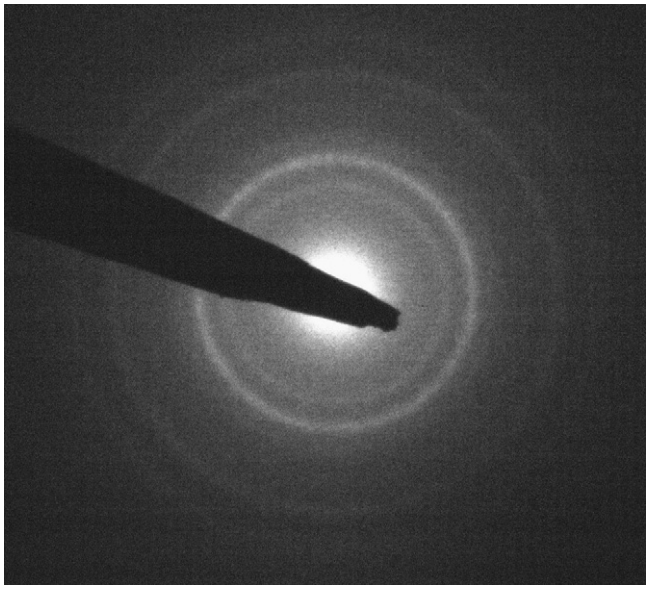

Fig. 4. Electron diffraction pattern of Co–P catalysts electroless deposited from Co–P bath of pH 12.5 at 80 °C (the amorphous and polycrystalline structure).

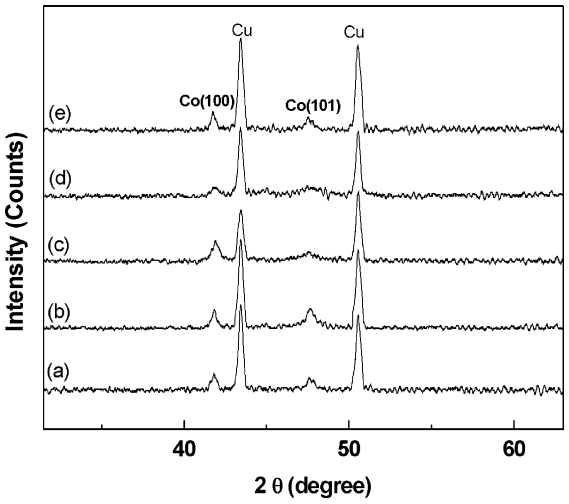

Fig. 5. XRD patterns of Co–P catalysts electroless deposited on Cu sheet from Co–P bath of (a) pH 10, (b) pH 11, (c) pH 12, (d) pH 12.5, and (e) pH 13 at 80 °C.

3.2. Effects of temperature in Co–P bath

The effects of bath temperature on the surface morphologies of the Co–P catalysts electroless deposited on a Cu substrate in a Co–P bath at pH 12.5 were examined (Fig. 7). The weight of the Co–P deposits is 1.25 mg cm^{-2} for all the Co–P catalysts. The Co–P catalyst, which shows a duplex layer structure with outer spherical Co–P particles on an inner flat Co–P layer, is formed on the Cu in the bath at 50 °C. Moreover, micro-cracks are detected on the flat Co–P layer. These are caused by the high residual stress within the layer. When the bath temperature is increased from 50 to 90 °C, the number of the Co–P crystals decreases gradually. It appears, however, that the surface morphologies of the Co–P catalysts are less sensitive to the bath temperature than to the bath pH. In addition, the chemical composition of the Co–P catalysts is almost the same with Co–8–9 at.% P, irrespective of the bath temperature.

XRD patterns of the Co–P catalysts electroless deposited at different temperature are presented in Fig. 8. For the catalysts

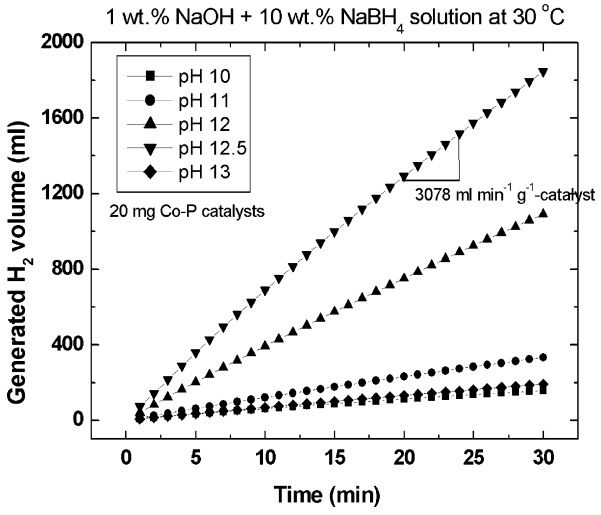

Fig. 6. Effects of pH in Co–P bath on hydrogen generation properties of Co–P catalysts deposited from Co–P bath of pH 10–13 at 80 °C.

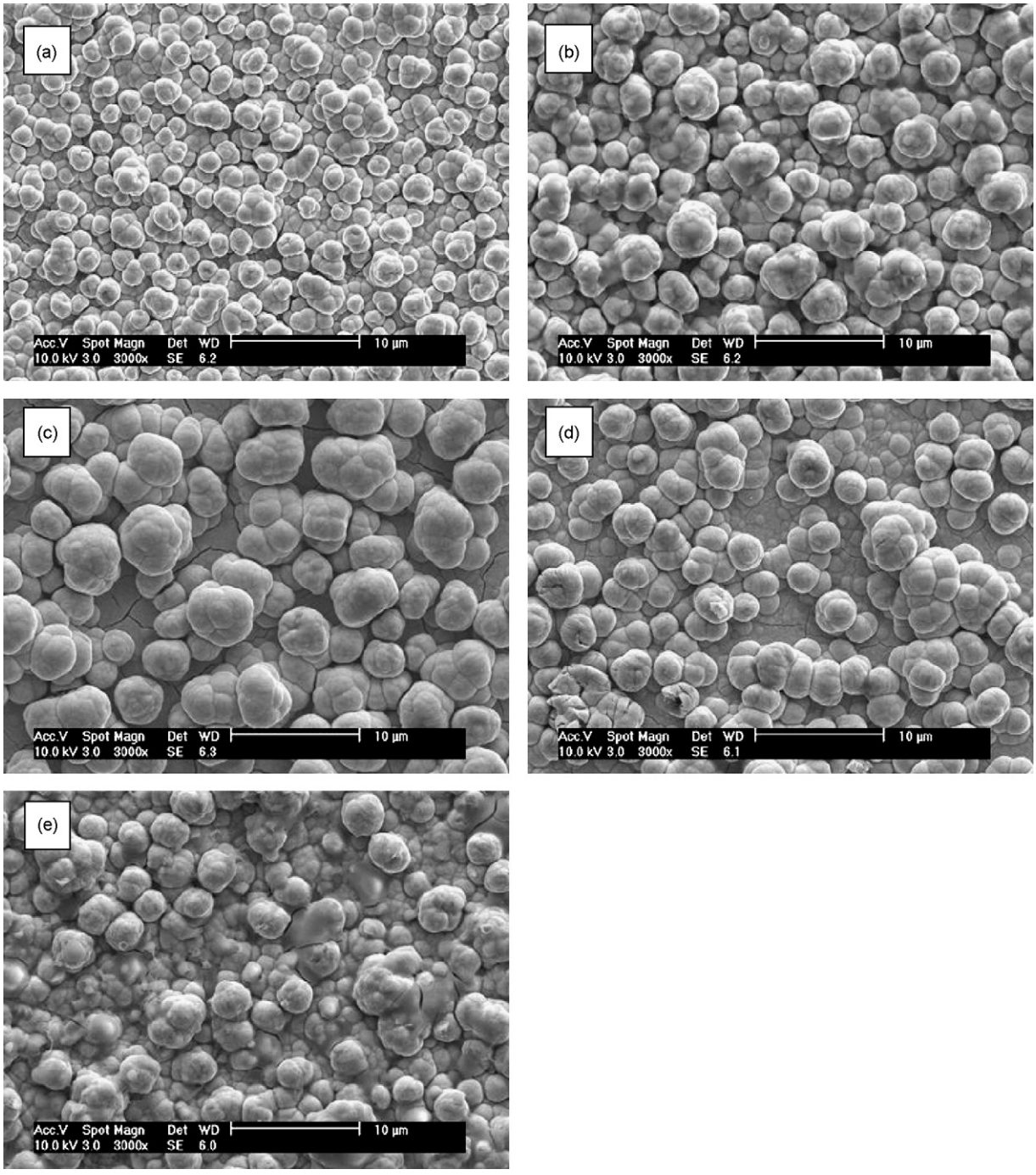

Fig. 7. SEM surface images of Co–P catalysts electroless deposited from Co–P bath at (a) 50 °C, (b) 60 °C, (c) 70 °C, (d) 80 °C, and (e) 90 °C at pH 12.5.

deposited at 50 and 60 °C, the (1 0 0) plane of the HCP Co phase is detected, and the broad peak indicates that the Co phase has a polycrystalline structure and its crystal size is very small. As seen in Fig. 3, however, the peaks related to the Co–P compound phase are not detected, which demonstrates that the Co–P compound is amorphous. When the temperature is increased to 70 °C, the peak intensity of the Co(1 0 0) plane is slightly decreased. With a further increase in the temperature to 90 °C, the Co(1 0 1) plane as well as the (1 0 0) plane are detected and the intensity of the Co peaks increases again. The crystal size Co–P catalyst formed at different bath temperatures were calculated by Scherrer's equation and are presented in Table 2. The results clearly show that the largest Co crystal size of 8.1 nm is obtained at 90 °C.

The effects of bath temperature during electroless deposition on the hydrogen generation properties of the Co–P catalysts in a

Table 2
Size of Co crystals in Co–P catalysts electroless deposited from Co–P bath of pH 12.5 at 80 °C

Temperature of Co–P bath (°C)	Average Co crystal size (nm) measured from HCP Co(1 0 0), (1 0 1) peaks by Scherrer's equation
50	–
60	6.0
70	4.2
80	5.0
90	8.1

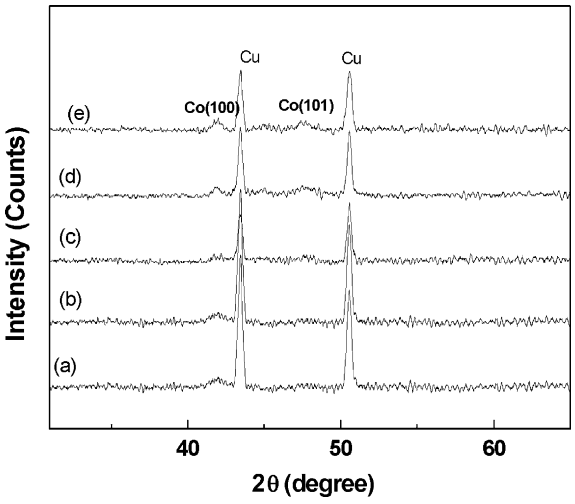

Fig. 8. XRD patterns of Co–P catalysts electroless deposited on Cu sheet from Co–P bath at (a) 50 °C, (b) 60 °C, (c) 70 °C, (d) 80 °C, and (e) 90 °C at pH 12.5.

solution of 1 wt.% NaOH and 10 wt.% $NaBH_4$ at 30 °C are presented in Fig. 9. As the temperature is increased from 50 to 60 °C, the hydrogen generation rate of the Co–P catalysts rises from 2584 to 3300 ml min^{-1} g^{-1}-catalyst. The hydrogen generation rate of the Co–P catalysts deposited at 70 and 80 °C is almost same as that at 60 °C. When the temperature is further increased to 90 °C, however, the hydrogen generation rate significantly decreases to 2300 ml min^{-1} g^{-1}-catalyst.

From the above results, it is revealed that Co–P catalysts with smaller crystalline Co have a higher hydrogen generation rate, as suggested by the dependence of the catalytic activity on the pH of the Co–P bath in Section 3.1. The Co–P catalyst electroless deposited in pH 12.5 baths at 60–70 °C have the smallest Co nano-crystals in the amorphous Co–P phase, and exhibit the best hydrogen generation rate of 3300 ml min^{-1} g^{-1}-catalyst in a solution of 1 wt.% NaOH and 10 wt.% $NaBH_4$ at 30 °C.

3.3. Hydrogen generation kinetics of Co–P catalysts

Fig. 10 shows the hydrogen generation kinetics of the Co–P catalyst in a solution of 1 wt.% NaOH and 10 wt.% $NaBH_4$ at various temperatures from 10 to 40 °C. The Co–P catalyst electroless

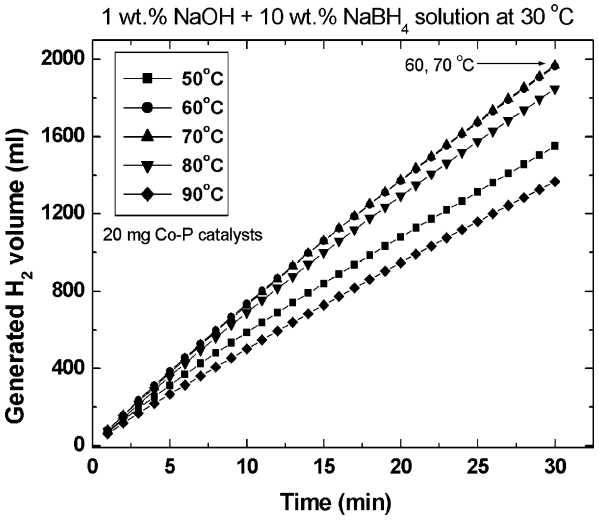

Fig. 9. Effects of bath temperature on hydrogen generation properties of Co–P catalysts deposited from Co–P bath at pH 12.5 at 50–90 °C.

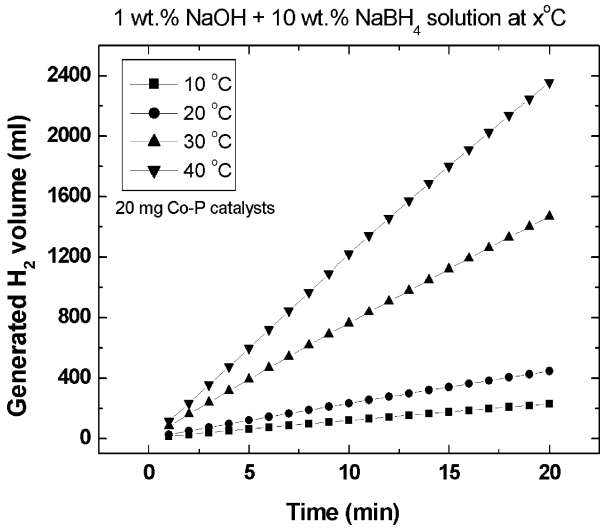

Fig. 10. Effects of the alkaline $NaBH_4$ solution temperature on hydrogen generation properties of Co–P catalysts electroless deposited from Co–P bath at pH 12.5 at 60 °C, in 10 wt.% $NaBH_4$ + 1 wt.% NaOH at x °C (x = 10, 20, 30, 40 °C).

deposited on Cu in a Co–P bath of pH 12.5 at 60 °C was used. With a rise in temperature from 10 to 40 °C, the hydrogen generation rate of the Co–P catalyst greatly increases from 570 to 5850 ml min^{-1} g^{-1}-catalyst. Moreover, the hydrogen generation reaction can be considered to be of zero order; the hydrogen generation rate is constant with reaction time, which indicates that the hydrolysis of $NaBH_4$ by the Co–P catalyst does not depend on the concentration of $NaBH_4$ remaining in the solution. The reaction rate equation can be written as follows

$$r = k_0 \exp\left(-\frac{E}{RT}\right) \quad (3)$$

where r is the reaction rate (ml min^{-1} g^{-1}-catalyst); k_0 is the reaction constant (ml min^{-1} g^{-1}-catalyst); E represents the activation energy for the reaction; R denotes the gas constant; T is the reaction temperature. Following Eq. (3), ln r versus $1/T$ is plotted in Fig. 11 using the data in Fig. 10. From the slope of the data, the activation energy for the hydrolysis of $NaBH_4$ by the Co–P catalyst is calculated to be 60.2 kJ mol^{-1}, which is close to the previously reported value of 56 kJ mol^{-1} for a Ru catalyst [6]. In addition, the activation energy

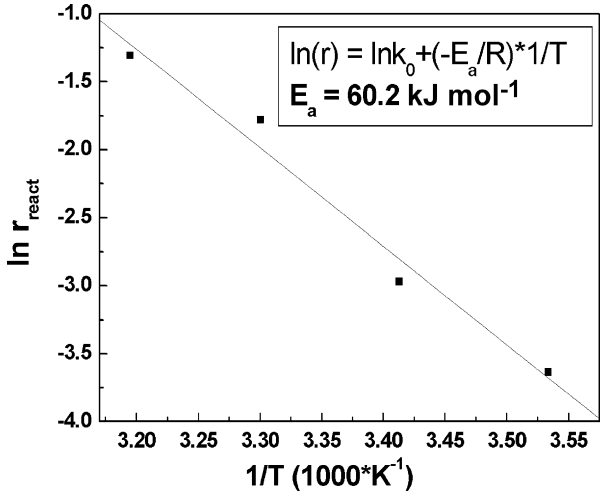

Fig. 11. ln r_{react} vs. $1/T$ plot obtained from data shown in Fig. 10 for hydrogen generation reaction using electroless-deposited Co–P catalysts from Co–P bath containing at pH 12.5 at 60 °C.

for the Co–P catalyst is smaller than that for pure metal catalysts (Co, 75; Ni, 71; Raney Ni, 63 kJ mol^{-1}) [10].

4. Conclusions

The effects of pH and temperature of the Co–P bath on the microstructures of electroless-deposited Co–P catalysts and their hydrogen generation properties in alkaline $NaBH_4$ solution have been investigated. The findings of this work are as follows:

1. Co–P catalysts, showing a duplex layer structure with outer spherical Co–P particles on an inner flat Co–P layer, are formed by electroless deposition in a chloride-based Co–P bath containing $H_2PO_2^-$ ions at pH 12.5. The Co–P catalysts consist of two different phases, namely, nano-polycrystalline Co particles in an amorphous Co–P matrix phase.
2. The hydrogen generation properties of the electroless-deposited Co–P catalysts in alkaline $NaBH_4$ solution depend largely on both the pH and the temperature of the Co–P bath. Both these parameters influence the size of the nano-crystalline Co particles in the amorphous Co–P matrix phase. The Co–P catalysts with smaller crystalline Co deliver higher hydrogen generation rates.
3. The electroless-deposited Co–P catalyst has much higher catalytic efficiency for the hydrolysis of $NaBH_4$ than the Co catalyst. For instance, the Co–P catalyst formed in the pH 12.5 bath at 60–70 °C gives a hydrogen generation rate of 3300 ml min^{-1} g^{-1}-catalyst in a solution of 1 wt.% NaOH and 10 wt.% $NaBH_4$ at 30 °C, which is 60 times higher than that of the Co catalyst. The activation energy for hydrolysis of $NaBH_4$ by the Co–P catalyst is calculated to be 60.2 kJ mol^{-1}.

Acknowledgements

This Research was performed for the Hydrogen Energy R&D Center, one of the 21st Century Frontier R&D Programs funded by the Ministry of Science and Technology of Korea.

References

[1] F. Mitlitsky, B. Myers, A. Weisberg, Hydrogen Energy Fuels 12 (1998) 56.
[2] L. Zaluski, A. Zaluska, J.O. Ström-Olsen, J. Alloys Compd. 253 (1997) 70.
[3] E. Akiba, H. Iba, Intermetallics 6 (1998) 461.
[4] P. Chen, X. Wu, J. Lin, K.L. Tan, Science 258 (1999) 91.
[5] Kreevoy, M.M. Jacobson, Ventron Alembic 15 (1979) 2.
[6] S.C. Amendola, P. Onnerud, M.T. Kelly, P.J. Petillo, S.L. Sharp-Goldman, M. Binder, J. Power Sources 85 (2000) 186.
[7] S.C. Amendola, S.L. Sharp-Goldman, M.S. Janjua, N.C. Spencer, M.T. Kelly, P.J. Petillo, M. Binder, Int. J. Hydrogen Energy 25 (2000) 969.
[8] Y. Kojima, K. Suzuki, K. Fukumoto, M. Sasaki, T. Yamamoto, Y. Kawai, H. Hayashi, Int. J. Hydrogen Energy 27 (2002) 1029.
[9] H.I. Schlesinger, H.C. Brown, A.E. Finholt, J.R. Gilbreath, H.R. Hoekstra, E.K. Hyde, J. Am. Chem. Soc. 75 (1953) 215.
[10] C.M. Kaufman, B. Sen, J. Chem. Soc., Dalton Trans. (1985) 307.
[11] C. Wu, F. Wu, Y. Bai, B. Yi, H. Zhang, Mater. Lett. 59 (2005) 1748.
[12] D. Hua, Y. Hanxi, A. Xinping, C. Chuansin, Int. J. Hydrogen Energy 28 (2003) 1095.
[13] B.H. Liu, Z.P. Li, S. Suda, J. Alloys Compd. 415 (2006) 288.
[14] S.U. Jeong, R.K. Kim, E.A. Cho, H.J. Kim, S.W. Nam, I.H. Oh, S.A. Hong, S.H. Kim, J. Power Sources 144 (2005) 129.
[15] K.W. Cho, H.S. Kwon, Catal. Today 120 (2006) 298–304.
[16] R. Tarozaite, M. Kurtinaitiene, A. Džiu:ve, Z. Jusys, Surf. Coat. Technol. 115 (1999) 57–65.
[17] I. Lucas, L. Perez, C. Aroca, P. Sanchez, E. Lopez, M.C. Sanchez, J. Magn. Magn. Mater. 290 (2005) 1513.
[18] B.D. Cullity, Elements of X-ray Diffraction, Addison Wesley, Indiana, 1978, 102.